ePDH
online.com

Credit: 1 PDH

Course Title:

Method for Aligning Facets in Large Concentrators

Approved for Credit in All 50 States
Visit epdhonline.com for state specific information including Ohio's required timing feature.

3 Easy Steps to Complete the Course:

1. Read the Course PDF
2. Purchase the Course Online & Take the Final Exam
3. Print Your Certificate

Method for Aligning Facets in Large Concentrators That Have Segmented Mirrors for Solar Thermal Applications

Sergio Vázquez y Montiel, Fermín Granados Agustín and
Lizbeth Castañeda Escobar

Additional information is available at the end of the chapter

Abstract

The high radiative flux solar furnaces already in operation, and the furnaces to be built in the future, have large concentrators consisting of multiple facets. It is, therefore, necessary to have an alignment procedure of the facets that guarantee the accuracy of alignment, allowing an alignment in a short time. This chapter presents a novel method for aligning the facets of a large concentrator, which uses a single optical system to achieve the required precision and the desired energy distribution in the focal plane. Simulation and experimental results obtained with our procedure show that the proposed alignment satisfactorily meets the specifications.

Keywords: Optical alignment, radiative flux, segmented concentrator, solar concentration, solar furnace

1. Introduction

Solar thermal energy (STE) is a form of solar energy to generate electrical energy or thermal energy for use in the residential and commercial sectors and in industry.

Concentrating solar power (CSP) plants use mirrors to concentrate the rays of sun and produce heat for electricity generation through a conventional thermodynamic cycle. These kinds of plants are candidates for providing the solar electricity needed within the next few decades.

According to thermodynamics and Planck's equation, the conversion of solar heat to mechanical work is limited by the Carnot efficiency, and then to achieve maximum conversion rates, the energy should be transferred to a thermal fluid or reactants at temperatures closer to that of the sun.

Solar radiation is a source of high temperature and energy. But for terrestrial use in average we have 1 kW/m^2. Therefore, it is an essential requisite for solar thermal power plants and high-temperature solar chemistry applications to make use of optical concentration devices that enable the thermal conversion to be carried out at high solar flux and with relatively little heat loss.

The high radiative flux solar furnace (HFSF) is the solar concentrator system with greater concentration ratio. This type of system uses large concentrators with dimensions of several meters, which cannot be constructed in one piece; they are built with multiple segments.

A key to these large concentrators operate efficiently is the alignment of the segments. This kind of concentrators has hundreds of segments that must be aligned with high precision and in a short time, until now; there is no known solution to this problem by the authors. The method that we propose in this chapter is a solution that was tested in the solar furnace high radiative flux of Mexico successfully.

The era of modern solar furnaces had started in the 1950s. Among the first furnaces built were the furnace of Arizona State College in the United States in 1956 [1] and the furnace of the Government Institute for Industrial Research in Japan in 1956 [2].

Several applications of the solar furnace focus on the study of properties such as expansion coefficients, emissivity, thermal conductivity, melting points [2], crystal growth, and purification of materials. Also began developing methods for the measurement of high temperatures in receivers [3] and the flux density of concentrated radiation [4]. The later have evolved calorimetric techniques [5, 6].

The combination of a stationary concentrator and a heliostat has come to be known as solar furnace. The advantage of this combination when compared with a parabolic dish directly tracking the sun is that the focus is stationary. Both concentrator and instrumentation can be placed indoors.

The estimated yearly average insolation in México is 5.5 kWh/m^2 per day higher than all other countries. For this reason, in Mexico a high radiative flux solar furnace, HFSF, was built to initiate the development of concentrating solar technologies for the production of solar fuels such as hydrogen. This development is part of a larger project known as "National Laboratory for Solar Concentration Systems and Solar Chemistry" [7].

The initial design considered an intercepted power of approximately 30 kW, with a target peak concentration of approximately 10,000 suns. A global standard deviation of the optical errors less than or equal to 4 mrad was chosen to reach such a goal. The optical design of the whole HFSF consists of a heliostat of 81 m^2 (9 m by 9 m), a shutter and a multifaceted concentrator of 409 spherical mirrors. Once the concentrator was built and aligned, it was verified that it generates a thermal power of 30 KW, with peaks of 18,000 suns (about 18,000 kW/m^2) and less than or equal to 10 cm in diameter sunspot.

The optical design of the concentrator of the new high radiative flux solar furnace is carried out through ray tracing simulation. In this large HSFS, the concentrator is a mirror with hundreds of facets and these facets must be aligned to achieve the desired energy distribution.

We consider the concentrator of HFSF formed with 409 mirror facets of hexagonal contour with a diameter of 40 cm each of them, each one being a spherical first surface mirror [8]. These facets are grouped in five sets of different focal length, placed on a spherical supporting structure, and with corrected orientations in order that the incident radiation on each facet is reflected to the same focus (see Figure 1 and Table 1) [8].

Group	Numbers of facets	Radius of curvature (mm)	Focal distance(mm)
A	85	7500	3750
B	104	8000	4000
C	130	8500	4250
D	64	9000	4500
E	16	9500	4750

Table 1. Number of facets in each mirror group, corresponding to different radii of curvature.
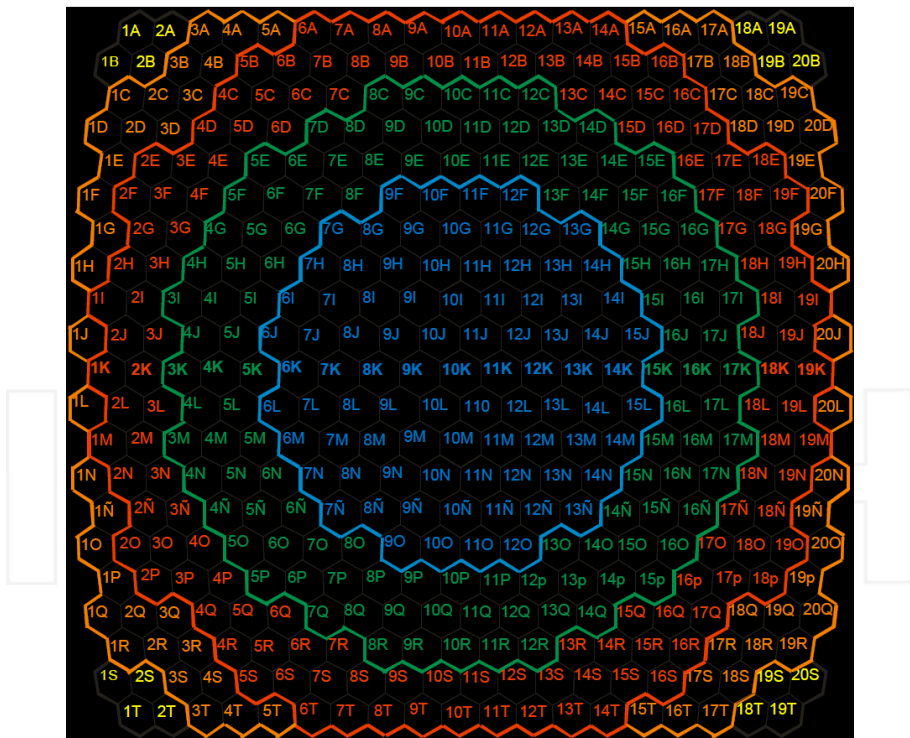

Figure 1. Arrangement of facets in the concentrator. Each color corresponds to a single focal length group.

To reduce manufacturing time and cost of the mirrors, they all have spherical surfaces. This means that the spatial and angular position of each mirror is calculated to compensate the aberrations and to reduce the spot size. Thus, the precise alignment of each mirror is essential for the proper operation of concentrator. Preliminary results of this method were reported by Vazquez et al [9].

In the optical design of the concentrator, the position of each mirror was calculated for collimated light. But it was not possible to use the sun as a light source for the alignment process due to the high temperature in the focal region (above 3000 K). The second reason for not using the sun in the alignment is that such a procedure would require the use of the HFSF heliostat to illuminate the concentrator. This would introduce an additional source of uncertainty, due to the imperfections in heliostat facet alignment and due to the sun tracking mechanism accuracy [9]. To decouple these sources of error from the process of concentrator facets alignment, a different procedure had to be proposed.

2. Alignment procedure facets

We proposed the following goals to be met by the alignment method:

- Use a light source other than the sun.
- The positioning of each facet can be achieved with the required accuracy.
- It is an easy method to implement.
- It works well in the environment where the concentrator is installed, independent of weather conditions.
- It does not require the use of the heliostat of the HFSF.

To fulfill those requirements, our method uses a quasi-point source, generated by a 25 mW HeNe laser (wavelength of 633 nm), together with a 60× microscope objective of 0.65 numerical aperture. This source is placed near the center of curvature of the set of mirrors to be aligned and the divergent light beam illuminates the concentrator. The light is reflected by each one of the mirror group. The reflection from each mirror forms a separate image at an observation screen. In the observation screen, the theoretical image produced by each mirror is calculated previously using the ray trace software. Alignment procedure is to match the actual spots with those calculated theoretically, by rotating the mirror around its supporting point. To this end, mirrors are attached to mechanisms enabling their movement in six degrees of freedom: displacement in three perpendicular directions and rotation around three axes. Each mirror is moved until the image matches the image generated theoretically. Figure 2 shows the optical arrangement used [9].

In Figure 3, a picture of the laser and the microscope objective used for generating the quasi-point light source is shown.

For each set of mirrors with the same radius of curvature, we place the point source generated by the optical arrangement of Figure 3 in a position near the center of curvature, then we need

to find the correct position of the observation screen, this position is where the spots are clearly defined and the spots are not overlapping each other.
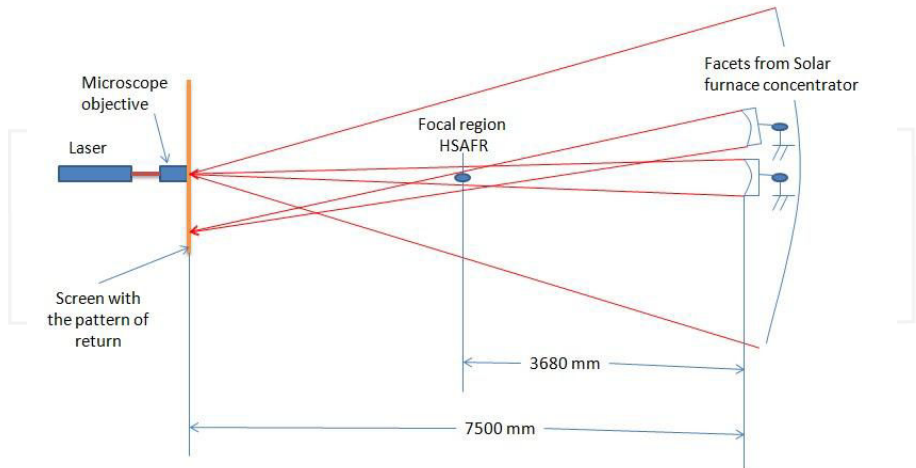

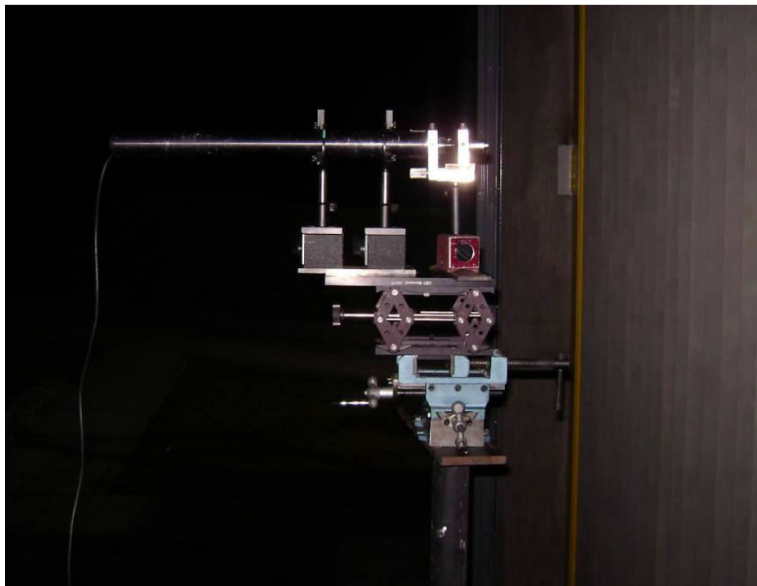**Figure 2.** Scheme with the optical arrangement for the alignment of the HRFSF facets.

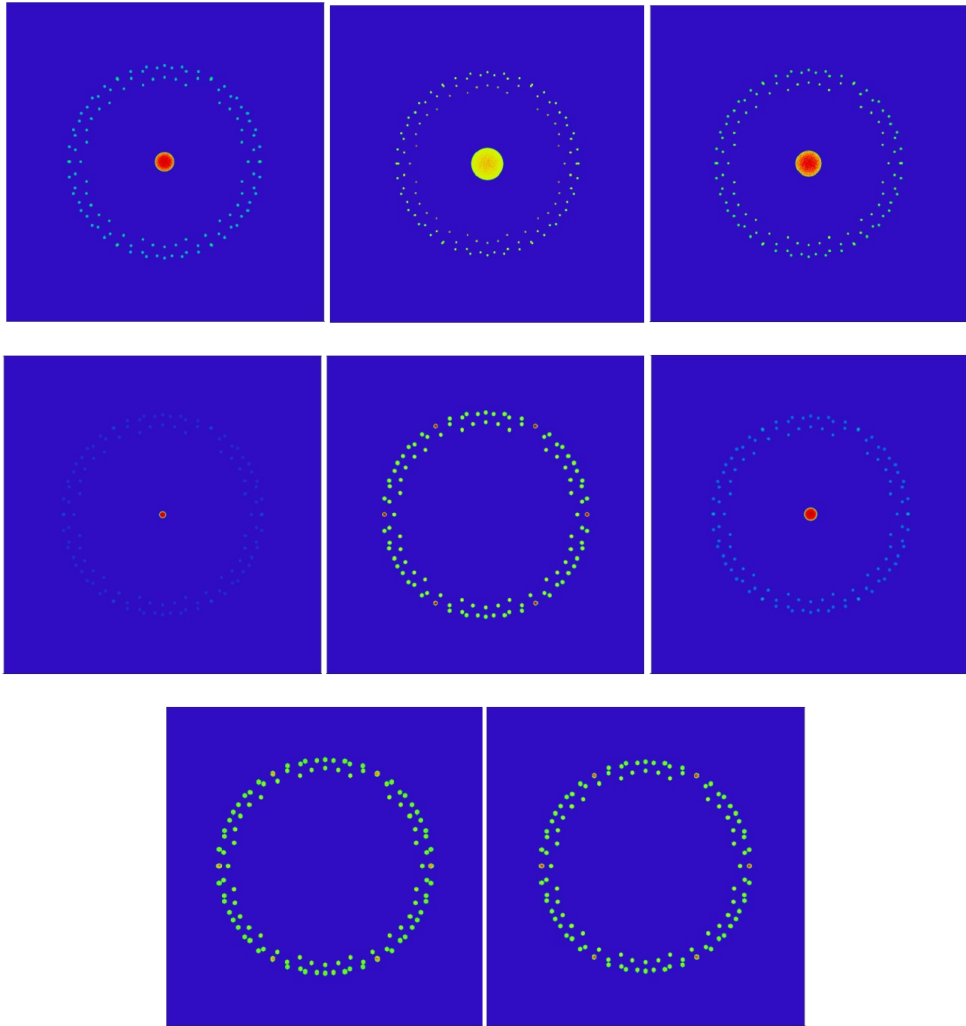**Figure 3.** Optical components for generating the quasi-point light source.

Figure 4. Simulation of images generated by mirrors with radius of curvature of 800 cm. Top left to bottom right, the images correspond to the following positions: –800 cm,– 802 cm,– 804 cm,– 806 cm, –808 cm,– 810 cm, –812 cm, and – 814 cm.

To establish the position of the observation screen, we made a simulation with the software ZEMAX OpticStudio by varying the position of the screen and observing the generated image. In Figure 4, we show simulation images for the mirror set of radius of curvature of 800 cm, the light source is placed at –810 cm and the screen was placed at positions –800 cm, –802 cm, –804 cm, –806 cm, –808 cm, –810, –812 cm, and –814 cm. As shown, the size and position of the spots change with the position of the screen. If the screen is placed in front of the light source,

there is a central spot causing noise during alignment and with this the intensity of the spots is reduced; however, if the screen is positioned behind the light source, the central spot disappears.

Figures 5 and 6 show the theoretically calculated alignment screens and mirrors corresponding to two sets of mirrors.

In Figure 7, a picture with the real spots on the alignment screen is shown. In the picture the spots generated by the mirrors with radius of curvature of 8500 mm and 9000 mm can be appreciated.
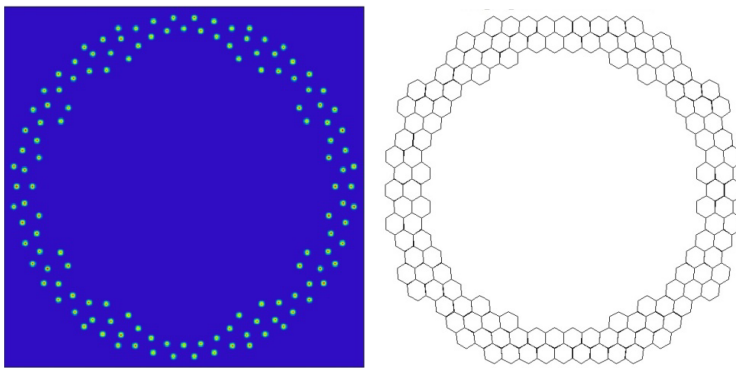

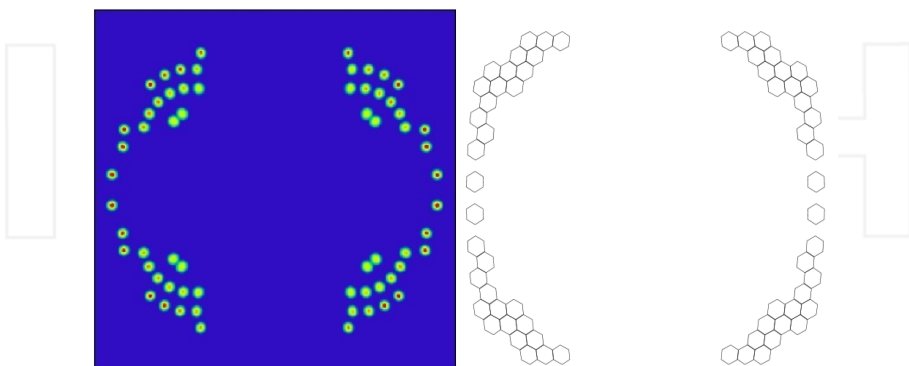**Figure 5.** Screen and mirrors corresponding to 850 cm curvature radius.

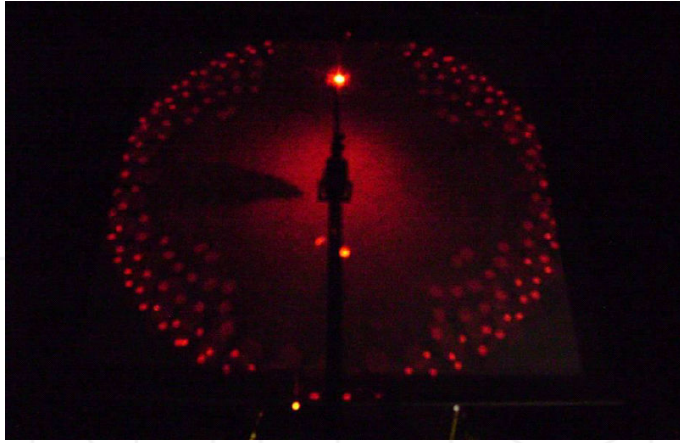**Figure 6.** Screen and mirrors corresponding to 900 cm curvature radius.

Figure 7. Picture with the real spots on the alignment screen [9].

3. Experimental results

After applying the alignment procedure for each of the concentrator mirrors, different tests were conducted to evaluate the accuracy of alignment. The first test was qualitative; the objective of this test was to observe the images of objects reflected by the concentrator [9]. As you can see, the images display excellent continuity and quality as a result of the alignment of the facets. It is a very good indication of the proper alignment of facets, see Figure 8.

Figure 8. Images reflected in the hexagonal facets after the alignment process [9].

For the second test, we use the 81 m² heliostat in conjunction with the concentrator, and the sun as a source of light. A water-cooled Lambertian target was positioned on the focal plane, and pictures of the solar image produced by the HFSF were taken with a charge-coupled device, CCD, camera [9], as can be seen in Figure 9.
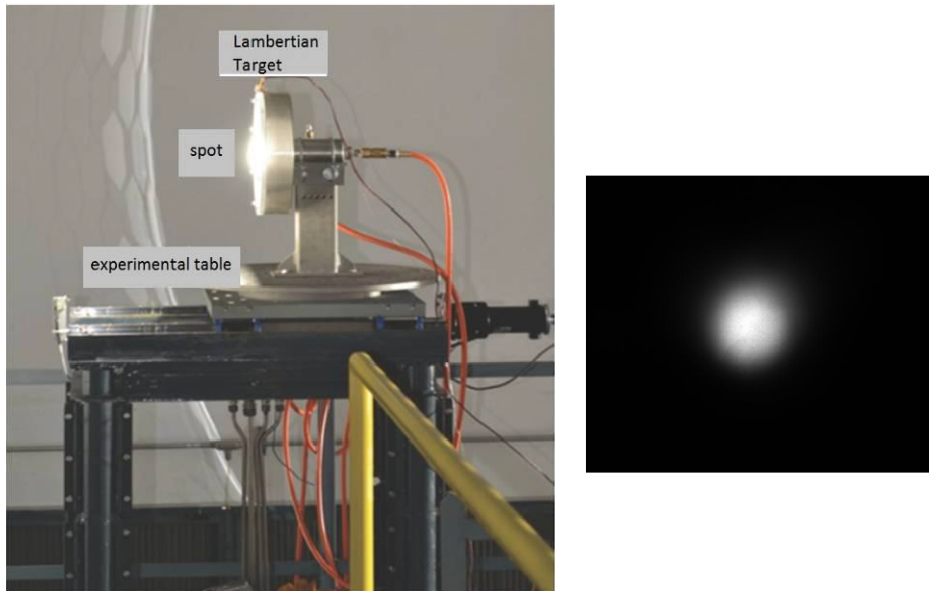

Figure 9. Water-cooled Lambertian target and example of solar image on the target.

To obtain the spot size and the distribution of irradiance we use MATLAB® software. With the results we estimate a spot diameter of 8 cm, and that 90% of the energy falls into a diameter of 6 cm. Comparing these results with ray tracing simulations, we conclude that our alignment procedure meets all requirements and that the standard deviation of the global optical error is of 2.7 ± 0.2 mrad.

Figure 10 shows an example of experimental image, the following steps to process the image and the resulting irradiance profile from the computer code.

The images obtained were compared with the results of the ray-tracing program called Tonalli [10]. The code calculates the irradiance flux on a focal plane using the convolution technique. We assume that the error distribution corresponds to a bidimensional Gaussian distribution characterized by a global standard deviation. The sun's model was taken from a standard solar radiation cone [10].

The images from CCD camera were analyzed, and we compared the profiles of irradiance in two orthogonal directions (horizontal and vertical) against the theoretical profile obtained for the global optical error, which gave the best fit with the experimental curve.

Image	Optical error, horizontal profile (mrad)	Optical error, vertical profile (mrad)
Image 1	2.8	2.8
Image 2	2.8	2.8
Image 3	2.8	2.4
Image 4	2.8	2.2

Table 2. Estimated optical error from different experimental images

Figure 11 shows an example of graphs obtained for the optimal adjustment in the horizontal and vertical image for first image as an example. Table 2 shows the summary of the results obtained with four images captured at different times. As you can see from the values in Table 2, the optical errors are consistent and repeatable; therefore, we can conclude that the global
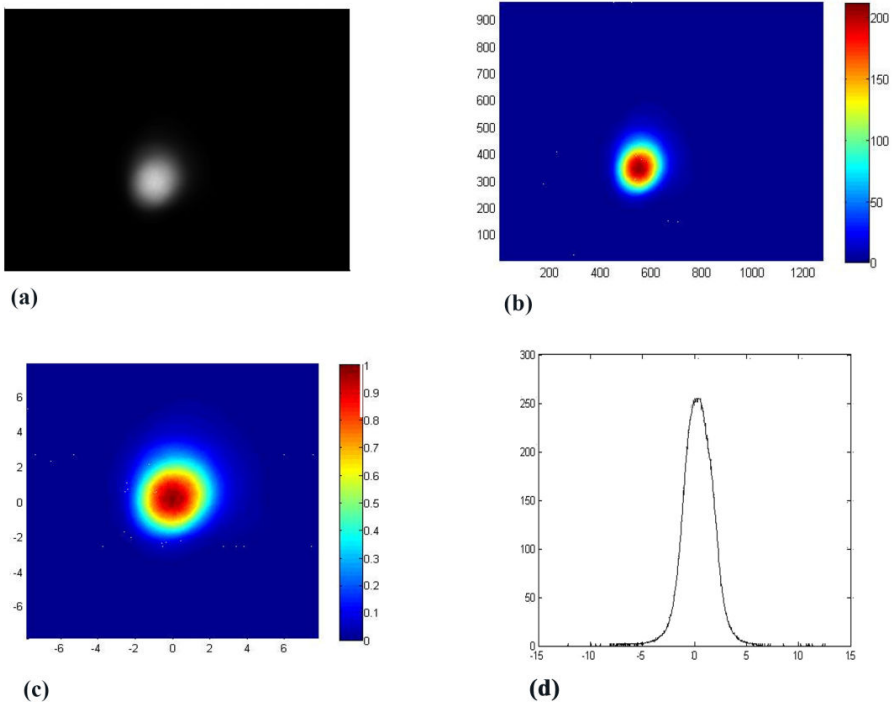

Figure 10. In (a) CCD picture from spot at the receiver at the focal point. (b) Picture translated to the computer for processing. The units of the image frame are mm. The values of the color scale must be multiplied by 100 W. (c) Image centered and processed. The units of the image frame are cm. The color scale is normalized. (d) Irradiance profile from the solar spot. The horizontal axis is cm and the vertical should be multiplied by 100 W.

optical error is approximately 2.7 ± 0.2 mrad. It is important to note that this error does not include the tracking error of the heliostat along the solar day.

Figure 11 only presents the adjustment in particular directions from the images, but they cannot show the symmetry of the image compared to those expected theoretically. Figure 12 shows theoretical and experimental comparison of the contours of the irradiance distributions at the receiver for image 1. To construct Figure 12, a particular level of irradiance is set in the experimental and the theoretical image, the curve formed by points with the same irradiance value is a contour. Each color in Figure 12 corresponds to a different level of irradiance in the image. There are two curves with the same color, corresponding to the experimental and theoretical images. The experimental and theoretical distributions were normalized with respect to the peak.
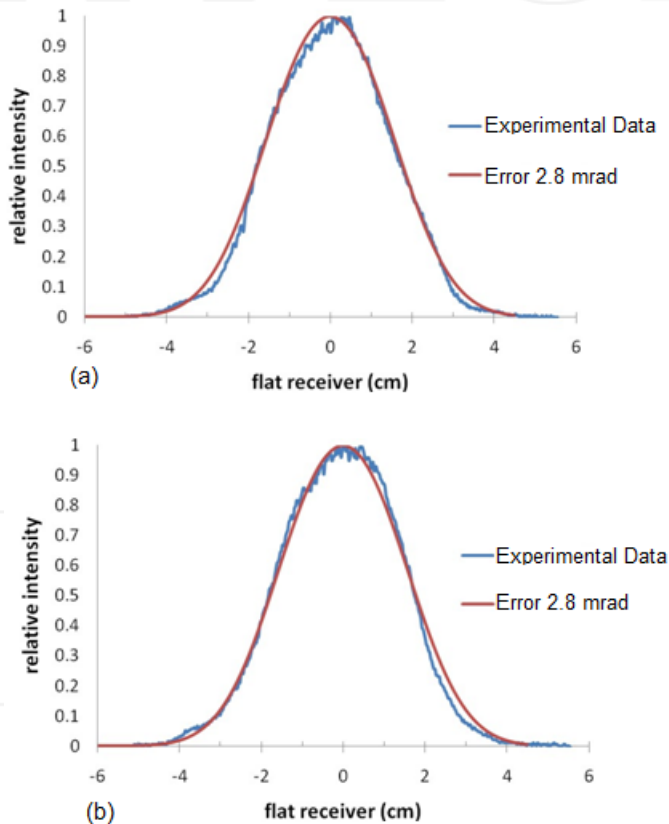

Figure 11. Comparison of experimental and theoretical irradiance profiles for image 1. (a) Vertical profile. (b) Horizontal profile.

Figure 12 shows a relative good correspondence with experimental results except in the lower contour in which there is a deviation from the circular shape of the image.
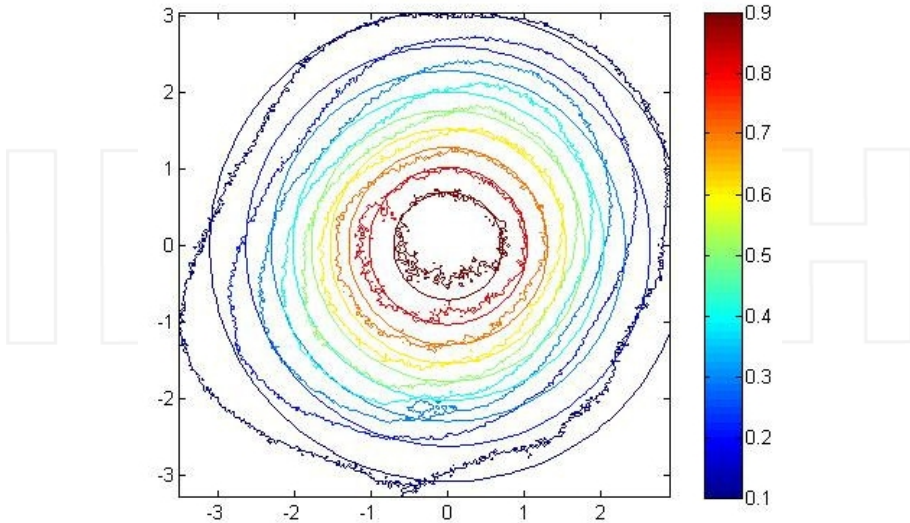

Figure 12. Comparison of experimental and theoretical contours, for image 1. The color scale units are Watts and is normalized.

4. Alignment tolerances of the method

Although the method has only geometric bases and their implementation requires fewer optical elements and sophisticated software is not required to process data as if it require other techniques, the results of the Section 3 shows that the alignment is within specified tolerances. To understand why the proposed method gives such good results, the following analysis was performed.

The optical concentrator design considers that the light source is at infinity and has the angular size of the sun, with these considerations the positions of each of the segments were defined for maximum concentration. However, in the alignment method the light source is near the center of curvature of each group of mirrors. Therefore, it is necessary to know as alignment errors are transformed into errors in the image.

In the mirror set of 850 cm of radius of curvature, we select one of them and will apply rotations around the X-axis in the range of –0.25 degrees to 0.25 degrees, and we calculate changes in image position for each angle. Figure 13 shows a graph of the results, the behavior is almost linear, and follows the following equation:

$$y = 22.737x + 0.116, \tag{1}$$

where the variable x represents the rotation angle of the mirror and variable y represents the displacement of the image position.

As the diameter of the spot generated by the mirror is 4 mm, the maximum possible error in the alignment process corresponds to a displacement of 4 mm and this corresponds to a mirror rotation 0.012 degrees.
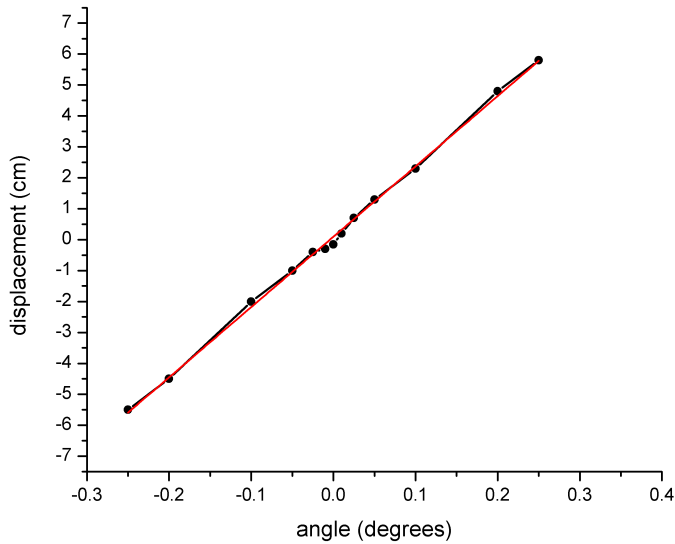

Figure 13. Image shift as a function of rotation of the mirror in the process of alignment. The dots (black) are the measured data and the solid line (red) corresponds to the fit of the data.

Figure 14 shows the ideal spot position without rotation and the spot position generated by applying a 0.01 degree rotation, during the alignment process. It is clear that this could be the maximum possible error.

Using the same mirror, but considering the sun as light source, we apply rotations of the mirror in a range of 0.01 degrees to 0.1 degrees, and we calculate the displacement of the image, the results are shown in the graph of Figure 15. As you can see, the behavior is almost linear and follows the following equation:

$$y = 32.757x - 0.0006, \tag{2}$$

where the variable x represents the rotation angle of the mirror and variable y represents the displacement of the image position.
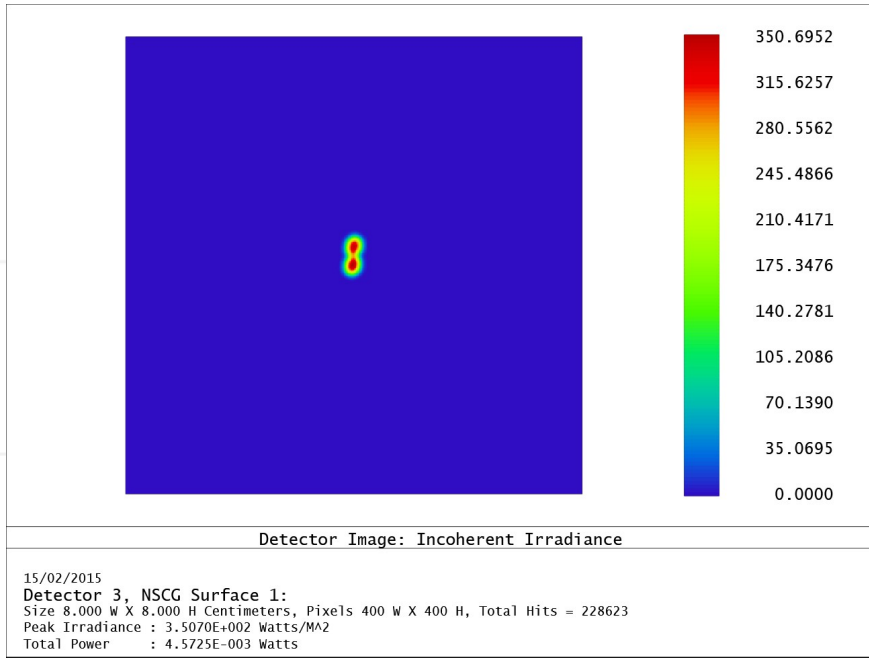
Figure 14. The ideal spot position and spot displaced by a rotation of 0.01 degrees.
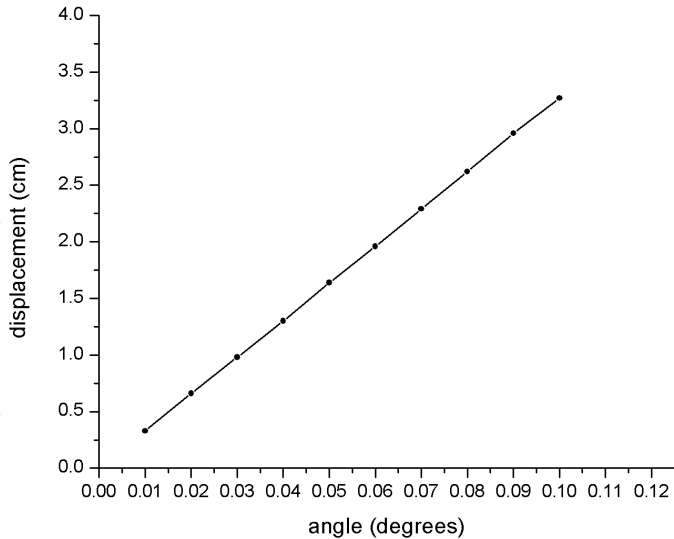

Figure 15. Image shift as a function of rotation of the mirror with the sun as a light source. The dots are the measured data and the solid line corresponds to the fit of the data.

Therefore, a rotation of 0.12 degrees involves a displacement of 0.39 cm. As the sun's image generated by the mirror is 6 cm, this displacement would generate a maximum error of 13% and the image would have a diameter of 6.78 cm corresponding to the specifications as an 8 cm in diameter is desired. Similar results are obtained with rotations about the *Y*-axis and mirror displacements along the three axes.

5. Conclusions

We have presented a novel method for aligning facets of segmented mirrors for applications of concentrating solar power. This is a method that requires only three optical components: it is cheap and easy to implement and can be used during day and night because the light source is a laser.

We showed that the proposed method allows the alignment of the segments and obtained the specifications with relative simplicity. We obtained the maximum errors that can occur in the alignment process and we find that the method generates errors tolerable without complicated computer programs.

After the alignment process, we used different tests to verify the actual operation of the concentrator and all tests showed a performance that exceeds expectations, demonstrating the viability of the proposed method.

Finally, if CCD cameras and image processing software are used, this method could be used to align the segmented mirror facets as used in large telescopes.

Author details

Sergio Vázquez y Montiel[1*], Fermín Granados Agustín[2] and Lizbeth Castañeda Escobar[3]

*Address all correspondence to: gatoangora2000@yahoo.com.mx

1 Polytechnic University of Tulancingo, México

2 National Institute of Astrophysics, Optics and Electronics, México

3 Instituto Tecnológico Superior de Xalapa, México

References

[1] Kevane, C.J., 1957. Construction and operation of the Arizona State College solar furnace. Solar Energy 1, 99–101.

[2] Hisada, T., Mii, H., Noguchi, C., Noguchi, T., Hukuo, N., Mizuno, M., 1957. Concentration of the solar radiation in a solar furnace. Solar Energy 1, 14–18.

[3] Brenden, B.B., Newkirk, H.W., S.H., 1958. A study of temperature measurement in a solar furnace. Solar Energy 2, 13–17.

[4] Loh, E., Hiester, N.K., Tietz, T.E., 1957. Heat flux measurements at the sun image of the California institute of technology lens-type solar furnace. Solar Energy 1, 23–26.

[5] Pérez-Rábago, C.A., Marcos, M.J., Romero, M., Estrada, C.A., 2006. Heat transfer in a conical cavity calorimeter for measuring thermal power of a point focus concentrator. Solar Energy 80, 1434–1442.

[6] Estrada, C.A., Jaramillo, O.A., Acosta, R., Arancibia-Bulnes, C.A., 2007. Heat transfer analysis in a calorimeter for concentrated solar radiation measurements. Solar Energy 81, 1306–1313.

[7] http://lacyqs.cie.unam.mx/es/index.php/instalaciones/horno-solar-de-alto-flujo-radiativo.

[8] Rivero-Rosas, D., Herrera-Vázquez, J., Pérez-Rabago, C. A., Arancibia-Bulnes, C.A., Vázquez-Montiel, S., Sanchez-González, M., Granados-Agustín, F., Jaramillo, O.A., Estrada, C.A. 2010. Optical design of a high radiative flux solar furnace for Mexico. Solar Energy 84, 792–800.

[9] Vázquez-Montiel, S., Pérez-Rabago C.A., Pérez-Enciso, R., Rivero-Rosas, D., Granados-Agustín, F., Arancibia-Bulnes, C.A., Estrada, C.A. 2011. Method for facets alignment for the high flux solar furnace at CIE-UNAM in Temixco, Mexico, First Stage. In: SolarPaces September 2011; September 2011; Granada Spain. 2011.

[10] Rivero-Rosas D., Pérez-Rabago C. A., Arancibia-Bulnes C. A., Pérez-Enciso R., Estrada C. A.. Concentration Images Profiles of the High-Flux Solar Furnace of CIE-UNAM in Temixco, Mexico, First Stage. In: SolarPaces September 2011 symposium; Granada Spain. 2011.